Original Article: Graphedin Structures Simultaneously Doped with Boron and Nitrogen in One Layer

Andi Brous

[1]*Department of Research and Development, UOP, Texas, U.S.A*

Use yor device to scan and read the article online

Citation Brous A. Graphedin Structures Simultaneously Doped with Boron and Nitrogen in One Layer. J. Eng. Indu. Res. 2021; 2(2):56-63.

doi 10.22034/jeires.2021.270715.1026

Article info:
Received: 28 September 2020
Accepted: 22 February 2021
Available Online: 20 March 2021
Checked for Plagiarism:
Dr. Sami Sajjadifar
Peer Reviewers Approved by:
Dr. Amir Samimi
Editor who Approved Publication:
Professor Dr. Mohammad Haghighi

Keywords:
Graphide structures, Atoms, Electrical conductivity, Semiconductor, Insulation

ABSTRACT

This study investigated and optimized graphene structures simultaneously doped with boron and nitrogen in a single layer. Finally, the best graphedine structures doped with a boron atom and a nitrogen atom were determined. In pure Graddine PDOS and DOS diagrams, only the p-orbitals play a major role around the Fermi region. In fact, the peaks around the Fermi region correspond to the p orbitals in the guide bar and the capacity bar. In general, capacitance and conduction bands are bands close to the Fermi level and determine the amount of electrical conductivity in solids. In the pure bilayer graphene strip structure, the zero Fermi energy level is in the energy gap range. The energy gap is completely open in the entire Brillouin area, and at the point of the direct energy gap, a magnitude (eV) of 0.141 is seen. If the energy gap values are classified according to conductivity, semiconductor and insulation, pure two-layer graphite can be considered a semiconductor with direct energy gap. If the energy gap is zero electron volts, the matter is conductive.

Introduction

The location of boron and nitrogen atoms in different places in structures 12 to 17 is as follows:

a) Structure 12: Boron instead of carbon sp^2 in the six-carbon ring (position I) and nitrogen instead of carbon sp in the eighteen-carbon ring (position II);

b) Structure 13: Nitrogen instead of carbon sp2 in the six-carbon ring (position I) and boron instead of carbon sp in the eighteen-carbon ring (position II);

c) Structure 14: Nitrogen instead of carbon sp2 in the six-carbon ring (position I) and boron instead of carbon sp;

The second acetylene group in the eighteen-carbon ring (position III);

d) Structure 15: Boron instead of carbon sp2 in the six-carbon ring (position I) and nitrogen instead of carbon sp;

The second acetylene group in the eighteen-carbon ring (position III);

e) Structure 16: Nitrogen instead of carbon sp in the eighteen-carbon ring (position II) and boron instead of carbon sp;

***Corresponding Author:** Andi Brous (andi.uop.2018@gmail.com)

The second carbon of the acetylene group in the eighteen-carbon ring (position III);
f) Structure 17: Boron instead of sp carbon in the eighteen-carbon ring (position II) and nitrogen instead of carbon sp [1-5].
The second carbon of the acetylene group in the eighteen-carbon ring (position III)

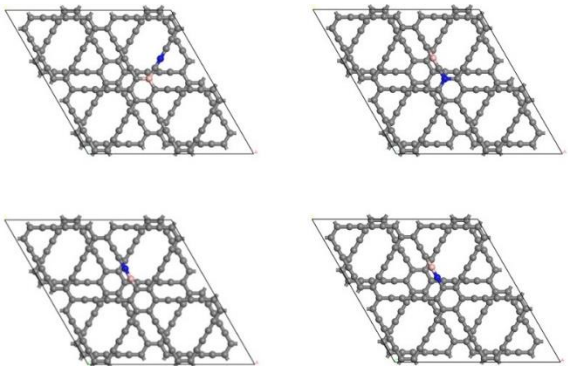

Figure 1. A view of the simultaneous doping of boron and nitrogen on a layer of two-layer graphite of structures 12 to 17

Investigation of The Effect of Adsorption of Hydrogen Cyanide Molecule on Graphene Doped with Boron and Nitrogen

According to the obtained results and diagrams of band structure and density of states, it was determined that the best graphedine structure doped with boron or nitrogen atoms is structure 10 and 11. To investigate the ability of hydrogen cyanide molecule to adsorb on these structures, the effect of adsorption of hydrogen cyanide molecule on different sites of these structures was investigated [6-9]. The absorption energy is obtained from the following Equation:

$$E_{Ads} = E_{(doped\ graphdiyne+HCN)} - E_{(doped\ graphdiyne)} - E_{HCN}$$

In this formula, at each site, the hydrogen cyanide molecule was placed horizontally and vertically from the ends of nitrogen and hydrogen on the structure to determine in which state a stronger interaction with the carbon structure occurs.

Investigation of Properties of Pure Bilayer Graphene

In this study, 2 2 2 two-layer graphite supercell cells were used for calculations. Figure (6) shows the band structure and density of partial states for the bilayer graphene supercell. In general, the number of electron states in an electron strip (conduction or capacitance) is very large [10-15].

The concept of state density is used to express the number of these states. Due to the symmetry, it is sufficient to obtain the state density in the Brillouin region, and then by it, the state density is obtained at all points of the crystal. Higher and sharper peaks in the DOS and PDOS diagrams indicate that there are more states in the corresponding energy. The Fermi surface is defined as the surface in space k where all the states inside it are occupied by capacitance electrons. All states outside this level are empty. There are two types of carbon atoms in the graphedine plate with sp and sp2 hybrids, due to which there are three types of sp-sp, sp-sp2 and sp2-sp2 bonds in graphene [16-18].

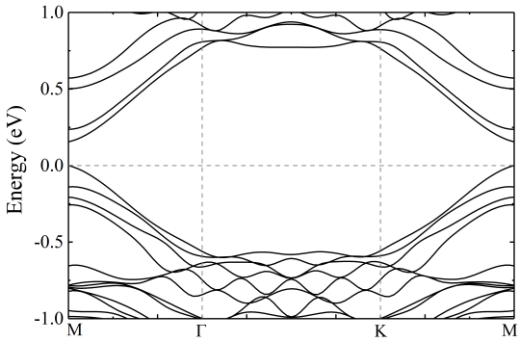

Figure 2. Two-layer graphite strip structure

The sp2-sp2 bond has the properties π and σ, where σ's share is related to the s, px and py orbitals, and π's share is related to the pz orbitals. The sp-sp bond is divided into one-part σ and two parts π. The σ segment, like the sp2-sp2 bond, depends on the s, px, and py orbitals, and the π segment, like the sp2-sp2 bond, binds to the pz orbitals. The other part π, which was absent in the sp2-sp2 bond, depending on px and py. The bond between sp-sp2 is also unique and depends only on the s, px and py orbitals [].

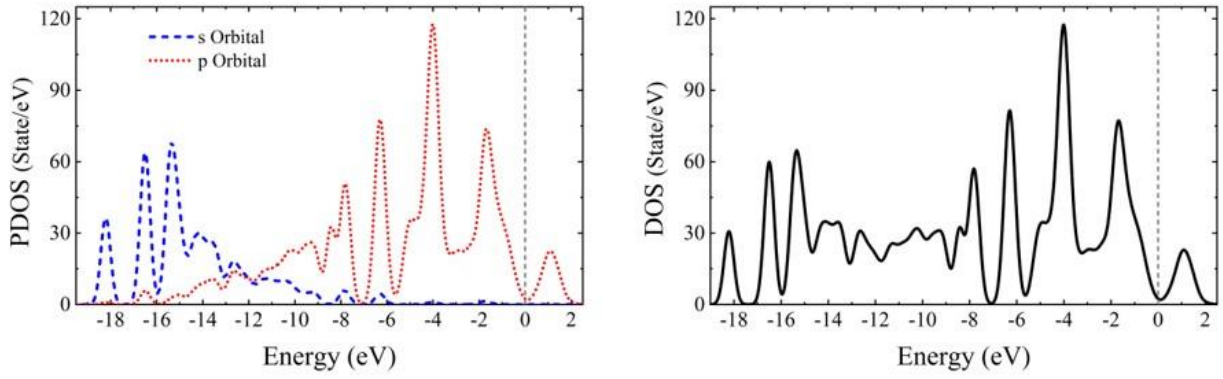

Figure 3. DOS and PDOS diagrams of pure bilayer graphite

Investigation of The Results of Placement of Hydrogen Cyanide Molecule on Pure 18-Carbon Graphite Ring of Pure Bilayer

To investigate whether the doping of boron and nitrogen atoms is an effective way to increase the energy of hydrogen cyanide adsorption on two-layer graphene, place the hydrogen cyanide molecule in the center of the eighteen-carbon ring, in the vertical direction from both nitrogen and hydrogen. Horizontal to the pure two-layer graphite, the plate was placed. The best position for adsorption of the hydrogen cyanide molecule in the center of the 18-carbon ring of structure 1 is horizontally parallel to the sp-sp bond on the ring. The amount of energy gap in this structure is reduced compared with structures doped with boron and nitrogen atoms (structures 10 and 11). The energy gap in pure bilayer graphene decreased to 1.155 eV and when hydrogen cyanide was adsorbed on the 18-carbon ring to 0.154 eV. The Fermi energy level in pure bilayer graphene reached -5.501 electron volts and reached 5.508 when hydrogen cyanide was adsorbed on the 18-carbon ring. The hydrogen cyanide molecule is calculated in structure 1 and the corresponding diagram is shown in Figure (4), the structure of pure bilayer graphene contaminated with hydrogen cyanide molecule in structure 1. In order to further investigate the electron properties of pure bilayer graphedine nanosheets contaminated with hydrogen cyanide molecule, DOS has been calculated for structure 1. The presence of the hydrogen cyanide molecule on the bilayer graphene compared with the pure bilayer graphene increased the density of the electron states. This is due to the fact that the overlap between the orbitals increases and as a result the charge transitions between the atoms also increase. Figure (9) shows the PDOS curve of adsorption of pure hydrogen cyanide molecule on pure bilayer graphene nanoplate. As can be seen, the available electron states around the Fermi surface are increased by the adsorption of hydrogen cyanide relative to the pure bilayer graphene [19-22].

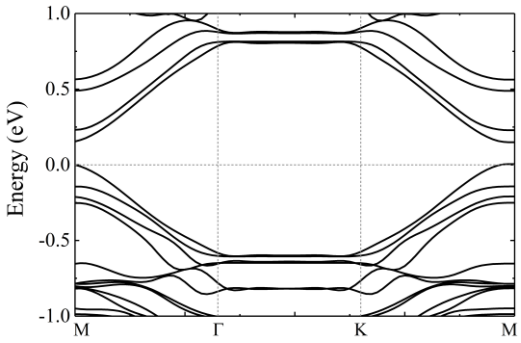

Figure 4. PDOS curve of two-layer graphene nanoplate contaminated with hydrogen cyanide molecule in structure 1

Investigation of The Results of Placement of Hydrogen Cyanide Molecule on The Structure of Pure Bilayer Graphene in The Center of a Carbon Six Ring

In the center of the carbon six ring, the hydrogen cyanide molecule was placed vertically and horizontally at a distance of 2 from the pure bilayer plate. The hydrogen cyanide molecule in structure 2 was placed vertically at the center of the carbon six ring horizontally from the two ends

of nitrogen and hydrogen. In Structure 2, the amount of adsorption energy was negative. The amount of absorption energy in the structure was 2 times -1.8269 electron volts, which shows that the doping of boron and nitrogen atoms on a pure two-layer graphene plate greatly reduces the amount of absorption energy. It also shows that this structure is not desirable in terms of energy and stability [23-25]. Pure bilayer is seen in graphene. In the carbon six ring, if the hydrogen cyanide molecule is horizontal, the adsorption energy is higher, and in the carbon six ring, the horizontal position is better. The amount of energy gap obtained in structure 2 is 0.161 electron volts. The reduction of the energy gap is due to the interaction between the atomic orbitals of the hydrogen cyanide molecule and the pure bilayer plate. Also, the amount of Fermi energy in structure 2 is 5.516 electron volts, which is reduced compared to -5.501 in pure two-layer graphene. In order to study the electron properties of two-layer graphite nanoparticles contaminated with hydrogen cyanide molecule, the band structure for pure bilayer graphedine contaminated with hydrogen cyanide molecule in structure 2 is calculated and the corresponding diagram is shown in Figure (5) [26-29].

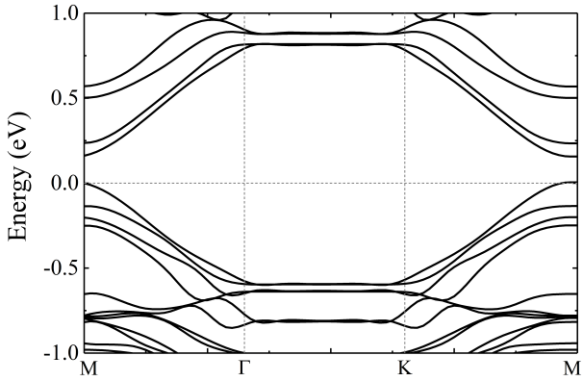

Figure 5. Structure of a pure bilayer graphene contaminated with a hydrogen cyanide molecule in structure 2

In order to further investigate the electronic properties of pure bilayer graphene nanoplate contaminated with hydrogen cyanide molecule, DOS is computed for structure 2 and its related diagrams. Contamination of the pure bilayer graphene plate with the hydrogen cyanide molecule increases the density of the electron states relative to the pure bilayer graphene [30-33].

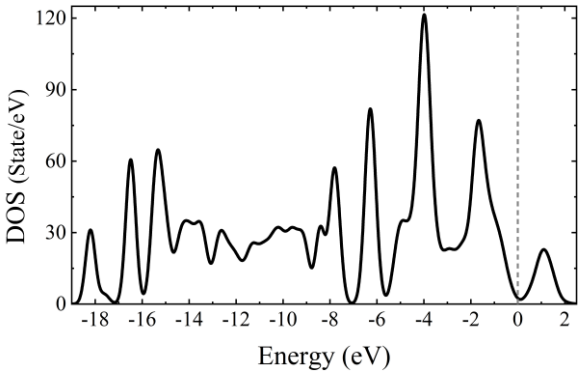

Figure 6. DOS curve of two-layer pure graphene nanoplate contaminated with hydrogen cyanide molecule in structure 2

The results obtained from the PDOS diagram show that the placement of the hydrogen cyanide molecule on the pure bilayer graphene increases the density of minor states near the Fermi surface and thus improves the conductivity properties relative to the pure bilayer graphene [33-35].

Evaluation of The Impact of Placement of Hydrogen Molecules on The Structure of Pure Bilayer Graphene In The Acetylene Group

In the acetylene functional group in graphene, the pure bilayer of the hydrogen cyanide molecule was placed vertically and horizontally at both ends of the hydrogen and nitrogen at a distance of 2 from the graphene plate of the pure bilayer. Nitrogen, hydrogen and horizontal ends were placed on the acetylene group. In Structure 3, the amount of adsorption energy was negative. The amount of absorption energy in the structure is 3 times 1.8011/electron volts, which is a negative value, indicating that the doping of boron and nitrogen atoms on a pure two-layer graphene plate greatly reduces the amount of absorption energy. It also shows that this structure is not a desirable structure in terms of energy and stability [38-40]. Pure bilayer is seen in graphene. In the carbon six ring, if the hydrogen cyanide molecule is horizontal, the adsorption energy is higher, and in the twelve-carbon ring, the horizontal position is better. The amount of energy gap obtained in structure 3 is 0.155 electron volts. The increase in the energy gap is due to the interaction between

the atomic orbitals of the hydrogen cyanide molecule and the pure bilayer plate.

Investigation of Monolayer Results of Two-Layer Graphene Structure with Boron Or Nitrogen Atoms

To investigate the doped interaction of boron and nitrogen atoms in a two-layer graphene plate, these atoms were each placed in three different positions on the graphene plate: Boron instead of carbon sp2 in the six carbon ring (position I) (structure 4), Nitrogen instead of carbon sp2 in the six carbon ring (position I) (structure 5), Boron instead of carbon sp in the ring Eighteen carbon (position II) (structure 6), nitrogen instead of carbon sp in the eighteen carbon ring (position II) (structure 7), boron instead of carbon sp attached to the second acetylene group in the eighteen carbon ring (position) III) (structure 8) and nitrogen instead of carbon sp attached to the second acetylene group in the eighteen carbon ring (position III) (structure 9). Examination of the results of the obtained structures shows that the binding energy in the presence of nitrogen atoms on the graphene plate, the two layers of structure 7 in which the nitrogen in position (II) is equal to 1808/8-electron volts and the best position for placing the boron atom on graphene Two-layer (I) which has a value of 1671/8 electron volts, having the lowest amount of nitrogen compared with other structures (Structure 4). Therefore, it can be said that the structure of a bilayer graphene that has one nitrogen atom in position (II) and one boron atom in position (I) is more stable. The energy gap decreases to zero electron volts after the nitrogen and boron atoms are doubled on a pure bilayer plate. This reduction in the energy band gap is due to the interaction between the orbitals of the bipolar atoms and the bilayer graphene nanoplate. The band gap is reduced from 0.141 eV for pure bilayer nanoparticles to zero for these six structures. According to the obtained band structure diagrams, the amount of energy band gap in the structures of 4 to 9 zero electron volts was obtained. These results show that, due to the doubling of the carbon atom with boron and nitrogen atoms on the bilayer graphene nanosheet, the energy level of the capacitance and conduction bands has changed significantly and due to the collision of the Fermi energy level with the capacity level or conduction energy gap, the value is zero. And the composition has found a quasi-metallic property.

Comparison of DOS diagrams of structures 4 to 9 shows that the doping of boron and nitrogen atoms at different sites has a significant effect on two-layer graphene DOS diagrams. The biggest change to the DOS graph is the bilayer doped with nitrogen atoms, with the graph moving more towards more negative energies. Of the three nitrogen-doped sites, structure 7 and among the three boron-doped sites, structure 4 has the lowest energy. As can be seen in the DOS diagram, in the structure of 7 peaks, more negative energy is transferred to the more negative ones. In fact, the doping of boron and nitrogen atoms causes a change in the DOS graph; Structure 5 Structure 4 Structure 7 Structure 6 Structure 9 Structure 8.

For a more detailed study, the PDOS curves of structures 4 to 9 are presented in Figure (8). As can be seen, only p-orbital states are available around the Fermi surface in pure bilayer graphite structure, while near the Fermi surface there are more available states in boron and nitrogen-doped structures. As a result, increasing the available densities improves the conductivity of doped graphene compared with pure graphene. Comparison of structures 4 to 9 with pure bilayer graphene shows that the doping of boron and nitrogen atoms at different sites has increased the density of the electron states.

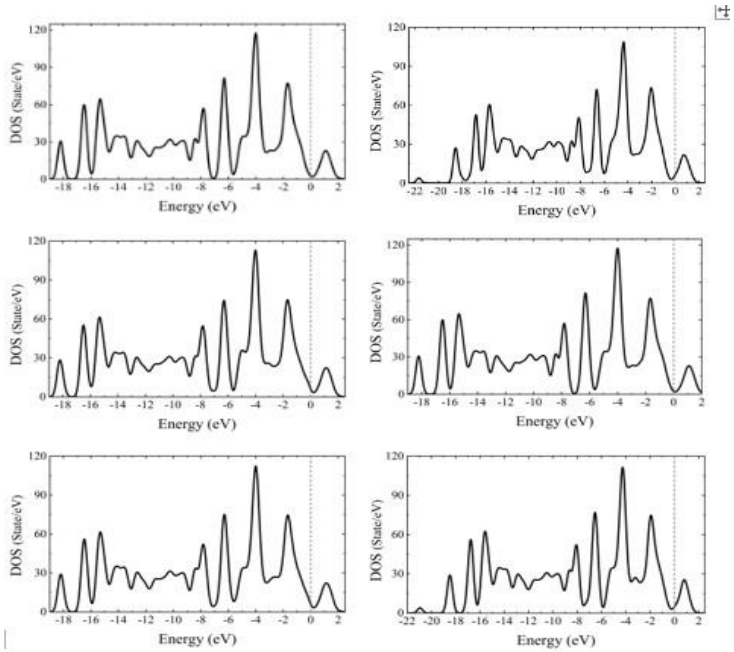

Figure 7. DOS curve of bilayer bilayer graphedine nanosheet with boron and nitrogen atoms at different doping sites, structure 4: B (I), structure 5: N (I), structure 6: B (II), structure 7: N (II), Structure 8: B (III), structure 9: N (III).

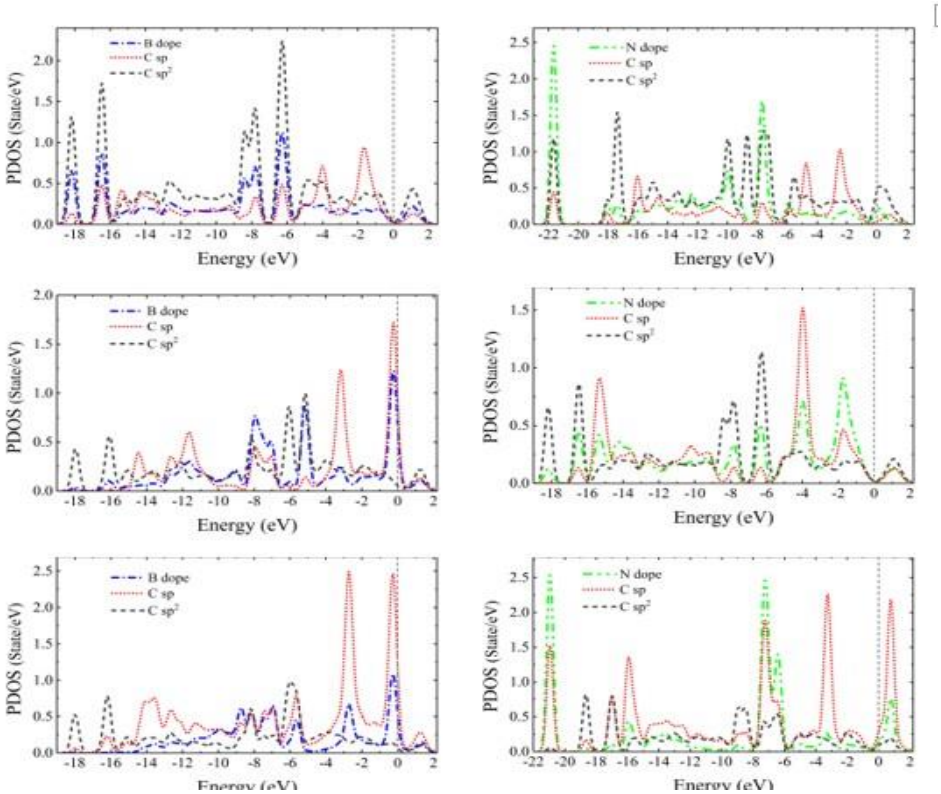

Figure 8. PDOS curve of a bilayer bilayer structure structured with boron and nitrogen atoms at different doping sites: Structure 4: B (I), structure 5: N (I), structure 6: B (II), structure 7: N (II), structure 8: B (III), structure 9: N (III).

Conclusion

In this paper, different structures of bilayer graphene and the effect of boron and nitrogen atoms in different locations of graphene bilayer nanoplate on its optical and electron properties were investigated. Also, the effect of hydrogen cyanide adsorption on pure bilayer graphene nanoparticles and graphene doped with boron and nitrogen atoms alone was studied and the general results are as follows:

1) When the hydrogen cyanide molecule is on a boron atom doped with boron atoms (structures 18 to 21), structure 18 has the shortest distance and the most negative amount of adsorption energy.

2) When the hydrogen cyanide molecule is horizontally and vertically of both nitrogen and hydrogen at different positions on a bilayer doped with nitrogen atoms, all structures 22 to 25 have zero energy gap.

3) In all cases where the hydrogen cyanide molecule is placed horizontally and vertically from both ends of nitrogen and hydrogen on a graphene nanoplate doped with boron atoms in different places, all structures 18 to 21 have zero energy gap.

4) Of all the structures in different states, the structures 18 and 22 have the highest absorption energy.

5) According to the results obtained in all doped structures, structures 10 and 11 are very effective sites for increasing the energy of hydrogen cyanide adsorption on graphene nanoplate.

6) Examination of band structure diagrams and DOS shows that the amount of energy gap is reduced after doping of boron and nitrogen atoms in two-layer graphene structures contaminated with hydrogen cyanide molecule. In general, contamination of the hydrogen cyanide molecule and the doping of boron and nitrogen atoms leads to an increase in the density of electron states near the Fermi surface, thereby increasing the conductivity of pure bilayer graphene nanosheets.

Reference

[1]. K. Lo Han, *Journal of Engineering in Industrial Research.*, **2021**, 2, 123-133

[2]. A. Ahmad, A. Sadrodin Reyazi, *Journal of Engineering in Industrial Research.*, **2021**, 2, 134-160.

[3]. B. Barmasi, *Journal of Engineering in Industrial Research.*, **2021**, 2, 161-169.

[4]. M. Amirikoshkeki, *Journal of Engineering in Industrial Research.*, **2021**, 2, 170-178.

[5]. M. Bagherisadr, *Journal of Engineering in Industrial Research.*, **2021**, 2, 179-185.

[6]. F. Zare Kazemabadi, A. Heydarinasab, A. Akbarzadeh, M. Ardjmand, *Artificial cells, nanomedicine, and biotechnology*, **2019**, 47, 3222-3230.

[7]. A. Samimi, M. Samimi, *Journal of Engineering in Industrial Research.*, **2021**, 2, 1-6.

[8]. A. Bozorgian, P. KHadiv Parsi, M.A. Mousavian, *Nashrieh Shimi va Mohandesi Shimi Iran*, **2009**, 27, 59-68.

[9]. A. Bozorgian, P. KHadiv Parsi, M.A. Mousavian, *Iranian Journal of Chemical Engineering*, **2009**, 6, 73-86.

[10]. A. Bozorgian, S. Zarinabadi, A. Samimi, *Journal of Chemical Review*, **2020**, 2 و 122-129.

[11]. A. Bozorgian, *Journal of Engineering in Industrial Research*, **2020**, 1, 99-110.

[12]. M. Bagheri sadr, A. Bozorgian, *International Journal of Advanced Studies in Humanities and Social Science*, **2020**, 9, 252-261.

[13]. A. Bozorgian, *International Journal of Advanced Studies in Humanities and Social Science*, **2020**, 9, 241-251.

[14]. E. Amouzad Mahdiraji, M. Sedghi Amiri, *Journal of Engineering in Industrial Research.*, **2021**, 2, 7-16.

[15]. M. Torkaman, FZ. Kazemabadi, *Oriental Journal of Chemistry.*, **2017**, 33, 197.

[16]. M. Pour Kiani, M. Pourjafari Jozam, M. Pourjafari Jozam, *International Journal of Advanced Studies in Humanities and Social Science*, **2020**, 9, 150-164.

[17]. S. Ketabi, A. Sadeghi, *International Journal of Advanced Studies in Humanities and Social Science*, **2020**, 9, 1-20.

[18]. S. Salehi-Kordabadi, S. Karimi, M. Qorbani-Azar, *International Journal of Advanced Studies in Humanities and Social Science*, **2020**, 9, 21-36.

[19]. M.R. Rahnama, M. Ajza Shokouhi, A. Heydari, *International Journal of Advanced Studies in Humanities and Social Science*, **2020**, 9, 37-49.

[20]. A. Bozorgian, *International Journal of Advanced Studies in Humanities and Social Science*, **2020**, 9, 229-240.

[21]. A. Bozorgian, N.M. Nasab, H. Mirzazadeh, *World Academy of Science, Engineering and*

Technology International Journal of Materials and Metallurgical Engineering, **2011** ,5, 21-24.
[22]. A. Bozorgian, *International Journal of Advanced Studies in Humanities and Social Science*, **2020**, 9, 205-218.
[23]. J. Mashhadizadeh, A. Bozorgian, A. Azimi, *Eurasian Chemical Communications*, **2020**, 2, 536-547.
[24]. Gabriel A. Ayeni, *Journal of Engineering in Industrial Research.*, **2021**, 2,17-21.
[25]. F. Zare Kazemabadi, A. Heydarinasab, A. Akbarzadehkhiyavi, M. Ardjmand, *Chemical Methodologies*, **2021**, 5, 135-152.
[26]. S. Hashem, *Journal of Engineering in Industrial Research*, **2021**, 2, 44-55.
[27]. A. Bozorgian, Z. Arab Aboosadi, A. Mohammadi, B. Honarvar, A. Azimi, *Eurasian Chemical Communications*, **2020**, 2 (3), 420-426.
[28]. Akhtarian zand, *Journal of Engineering in Industrial Research.*, **2021**, 2, 22-27.
[29]. K. Malmal, N. Shiri, *Journal of Engineering in Industrial Research.*, **2021**, 2, 28-35.
[30]. Z. Torabi, *Journal of Engineering in Industrial Research.*, **2021**, 2, 36-43.
[31]. Y. Kamyabi, M. Salahinejad, *International Journal of Advanced Studies in Humanities and Social Science*, **2020**, 9, 50-62.
[32]. S. Delavari, H. Mohammadi Nik, N. Mohammadi, A. Samimi, S.Y. Zolfegharifar, F. Antalovits, L. Niedzwiecki, R. Mesbah, *Chemical Methodologies*, **2021**, 5, 178-189.
[33]. A. Samimi, S. Zarinabadi, A.H. Shahbazi Kootenaei, A. Azimi, M. Mirzaei, *South African Journal of Chemical Engineering.*, **2020**, 31, 44-50.
[34]. A. Samimi, S. Zarinabadi, A.H. Shahbazi Kootenaei, A. Azimi, M. Mirzaei, *Eurasian Chemical Communications.*, **2020**, 2, 150-161.
[35]. A. Samimi, *Progress in Chemical and Biochemical Research*, **2020**, 3, 140-146.